Electronic structure of Nb-Ta (001) superlattices

1989 J. Phys.: Condens. Matter 1 6413

(http://iopscience.iop.org/0953-8984/1/36/009)

J. Phys.: Condens. Matter **1** (1989) 6413–6421. Printed in the UK

Electronic structure of Nb–Ta (001) superlattices

V R Velasco†, R Baquero‡, R A Brito-Orta‡ and F García-Moliner†
† Instituto de Ciencia de Materiales, Consejo Superior de Investigaciones Científicas, Serrano 123, 28006 Madrid, Spain
‡ Departamento de Fisica, Instituto de Ciencias, Universidad Autónoma de Puebla, Apdo. J-48, Puebla, Pue. 72570, Mexico

Received 31 October 1988, in final form 12 April 1989

Abstract. We have calculated the electronic band structure of Nb–Ta (001) superlattices by means of the surface-Green-function-matching method. An empirical tight-binding Hamiltonian including d orbitals and up to second-neighbour interactions is employed. The influences of the interactions at the interfaces and the relative thicknesses of the constituent materials on the superlattice spectrum are studied and discussed.

1. Introduction

In spite of the considerable attention currently being paid to the electronic structure of semiconductor superlattices, comparatively little time is devoted to the study of the electronic properties of metallic superlattices, partly owing to the lack of application of these systems to electronic devices but also because the complexity of the supercells tends to discourage realistic calculations. Nevertheless in these systems the ability to control layer thicknesses has already allowed studies of thickness and proximity effects on superconducting critical temperatures [1] and of the tunnelling density of states [2]. Self-consistent calculations for metal–metal superlattices up to (6, 6) thickness have been reported (see [3], and references therein) but the extension of these calculations to larger thicknesses would be extremely time consuming using a computer. For this reason it is useful to have other methods which allow simpler calculations, in spite of the loss of some accuracy, as long as the physical results remain meaningful and can be employed as a good first approximation. In some cases, when used appropriately, these approximate methods can give results which are in excellent agreement [4] with first-principles calculations. Empirical tight-binding (ETB) models are very useful for studying transition metals without enormous computational effort, in spite of their limited accuracy.

The surface-Green-function-matching (SGFM) method recently proposed for discrete crystalline superlattices [5, 6] is independent of the model and even of the physical nature of the elementary excitations under study. An interesting practical aspect of the method is that it separates the features of matching at each interface from those of propagation to the next interface across the slabs of the constituent materials. Thus the size of the matrices involved, and in particular of the secular matrix yielding the

0953-8984/89/366413 + 09 $02.50

Table 1. ETB parameters for the d orbitals used in our calculation for a Nb–Ta (001) superlattice.

	ETB parameter (eV)					
	$(dd\sigma)_1$	$(dd\pi)_1$	$(dd\delta)_1$	$(dd\sigma)_2$	$(dd\pi)_2$	$(dd\delta)_2$
Nb	−1.3783	0.7444	−0.1198	−0.6714	0.3626	0
Ta	−1.5813	0.8541	−0.1375	−0.7703	0.4161	0

superlattice states, is only doubled with respect to the single-interface case, irrespective of the size of the supercell.

By using an ETB model together with the SGFM method, we have a powerful predictive tool which can pinpoint the effects of the relative thicknesses of the constituents and/or changes in the interactions across the interfaces for a wide variety of superlattice thicknesses while avoiding the use of prohibitive amounts of computer time. This can compensate largely the limited accuracy of the ETB models and consequently the limited quantitative validity of the electronic structures thus obtained.

The ETB model employed here is described in § 2, the application to Nb–Ta (001) superlattices is discussed in § 3 and some conclusions are presented in § 4.

2. ETB Hamiltonian

The calculations were done with the SGFM method, which has been fully discussed elsewhere [5–8]. This involves the evaluation of matrix elements of the intervening Green functions, for which fast and efficient iterative algorithms can be used [9]. This makes the computational procedure rather efficient altogether [10].

As explained before, we shall try to study a wide range of thicknesses in metal–metal superlattices in order to build up a qualitative but fairly comprehensive picture. A study of this nature using *ab initio* methods would be extremely demanding on computer time and memory and is beyond our scope. The ETB Hamiltonians provide economic models, from the computational point of view, together with a reasonable accuracy compared with first-principles calculations [4, 10]. Because of this, we shall employ an ETB Hamiltonian for our study of the electronic structure of metal–metal superlattices. Since, in the electronic properties of transition metals, d electrons play the main role and the d-electron density of states overshadows the s and p densities around the Fermi level, and because we are interested in studying some general trends rather than aiming at accurate numerical values, we shall employ a two-centre parametrisation of the d bands using five non-zero parameters to describe the band structures of Nb and Ta. The tight-binding parameters used in our calculations are given in table 1. They have been obtained from the universal model in [11] which yields parameters very close to those obtained by fitting to known band structures [12].

Self-consistency can be included to a reasonable approximation in calculations based on ETB models [10, 13–17]. In the case of superlattices the local density of states (LDOS) can be evaluated by using recently developed methods of special points [18–19]. The non-self-consistent calculations yield extra charge densities $\delta\rho_n$ in different atomic layers. By imposing local charge neutrality everywhere, these are related to potential

shifts δV_n which one then adds to all diagonal elements of the Hamiltonian for the corresponding atomic layers. This simple method appears to be adequate for the intrinsic accuracy of the ETB models and has been successfully used for surfaces and interfaces of metals and semiconductors. On doing this, one would be correcting the energy value of the atomic level d_0 for each metal. As self-consistency was not included in the present calculation, we took $d_0 = 0$ for both metals.

A self-consistent calculation, even in this simple form, is a time-consuming numerical task which would be justified only if done together with a better basis and a specific fit including s and p orbitals in order to calculate some particular case. The purpose of this paper is only to study general trends and to demonstrate the capabilities contained in the method here employed so that more detailed calculations can be carried out if desired. The inclusion of self-consistency does alter some numerical results but does not change significantly the overall picture.

The present calculation employed a basis of five d orbitals per atom including second-nearest-neighbour interactions; so the principal layer contains two atomic layers. While self-consistency was not included for the reasons just explained, a fair estimate of the position of the Fermi level can be obtained by noting that surface effects (e.g. the change in the LDOS) in transition metals tend to be mainly confined to the surface layer [10]. By using the parameters of table 1 and the local charge neutrality condition for the interface layers of the Nb–Ta (001) interface the Fermi level is estimated to be at -1.1 eV [20]. It seems reasonable to assume that for the different superlattices to be studied here the Fermi level is not very far from this.

3. The Nb–Ta (001) superlattice

We have chosen the Nb–Ta (001) system because of the good matching of lattice parameters ($a_0 = 3.30$ Å for Nb and 3.30 Å for Ta) which has allowed the practical growth of superlattices from these constituent materials (see [21], and references therein). We assume perfect matching and ideal unreconstructed interfaces. The interactions at the interfaces are first taken as the mean of the bulk interactions of the two crystals and then changed in order to determine their influence on the electronic structure. It has been found for elastic waves [22, 23] and for phonons [24] that the relative thicknesses of the constituent slabs play an important role in the dispersion relation and the LDOS of the superlattice modes and, as a consequence, in their spatial confinement. We shall investigate this issue for the electronic structure of transiton-metal superlattices.

We have studied the electronic band structure along the growth direction [0, 0, 1] for $\kappa = (0, 0)$. The most significant feature is the existence of a number, depending on the slab thicknesses, of detached bands at very high and low energies, respectively, well above and below the folded bands. Their energies at the $\Gamma(0, 0, 0)$ and $Z(\pi/d(0, 0, 1))$ points are given in table 2 for a Nb–Ta (4, 4) superlattice. The corresponding dispersion relations as a function of k_z are given in figure 1.

Let (N, N') indicate a superlattice formed by alternating slabs of N (principal) layers of Nb and N' of Ta. We have studied all cases corresponding to N and N' equal to 2, 4, 8, 23, covering basically all limits of relative thicknesses, from low to high. We have found markedly different behaviours. For N' fixed, the highest and lowest bands are basically fixed at the Γ point and their eigenvalues are almost independent of N. This can be seen in table 3 for $N' = 4$ and in table 4 for $N' = 8$. These results can be easily

Table 2. Energies of the highest and lowest electron states at Γ and Z points in a Nb–Ta (001) (4, 4) superlattice.

	E (eV)	
	Γ	Z
Highest	4.73	4.73
Highest	4.67	4.65
Highest	4.39	4.42
Lowest	−5.89	−5.93
Lowest	−6.23	−6.19
Lowest	−6.34	−6.34

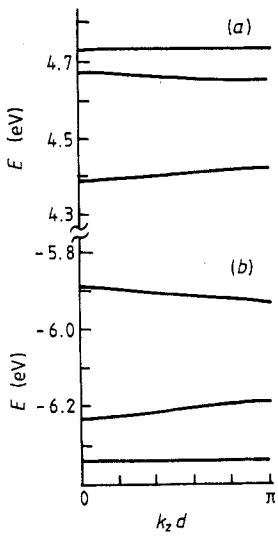

Figure 1. (*a*) Highest-energy and (*b*) lowest-energy bands along the Γ–Z direction for a Nb–Ta (001) (4, 4) superlattice.

understood by considering that, of the two bulk materials, Ta has the highest and lowest energies (4.85 eV and −6.5 eV, respectively) along the [0, 0, 1] direction, whereas for Nb the highest and lowest energies in that direction are 4.23 eV and −5.66 eV, respectively. The bands above 4.23 eV and below −5.66 eV are therefore forbidden in Nb. Thus these bands are associated with electronic states of Ta and a fixed number of Ta layers keeps the results for these bands unchanged even though the thickness of the Nb slab increases. On the contrary, when it is N' that increases, the high- and low-energy bands change and tend towards the corresponding Ta bulk spectrum. This physical picture is completed by looking at the spatial distribution of the spectral strength of states of the high- and low-energy bands. This is obtained in the standard way from the diagonal projections of G_s [8]. In figure 2, we give the spatial distribution of the spectral strength, i.e. the LDOS, for two of the highest and two of the lowest electron states at the Γ point of the (4, 8) superlattice.

All these states are basically confined to the Ta slabs, but in different ways. The highest mode at 4.81 eV in figure 2(*a*) tends to pile up towards the centre of the Ta slab, while the LDOS of the state at 4.68 eV (figure 2(*b*)) shows a marked dip at the centre.

Table 3. Energies of the highest and lowest electron states at Γ point in the Nb–Ta (001) (N, 4) superlattices (N = 2, 4, 8, 23).

	E (eV)			
	$N = 2$	$N = 4$	$N = 8$	$N = 23$
Highest	4.74	4.74	4.74	4.74
Highest	4.70	4.67	4.66	4.66
Highest	4.33	4.39	4.41	4.41
Lowest	−5.82	−5.89	−5.91	−5.91
Lowest	−6.28	−6.23	−6.21	−6.21
Lowest	−6.35	−6.34	−6.34	−6.34

The same behaviour is evident in figures 2(*c*) and 2(*d*) for the states at −6.28 eV and −6.44 eV, respectively. This behaviour is also found in the (4, 23) superlattice in spite of the fact that, when the thickness of the Ta slab increases, one would expect a tendency to reconstitute bulk Ta material.

Now, these states are well away from the Fermi level which, as explained in § 2, is expected to be in the neighbourhood of −1.1 eV. In order to see what happens in this energy range, we have studied the interval $-2\text{ eV} \leqslant E \leqslant 2\text{ eV}$ for the (4, 8) superlattice and found a variety of spatial confinements complementary to those shown in figure 2. This is illustrated in figure 3, which gives the LDOS of four states (at −1.52 eV, −1.38 eV,

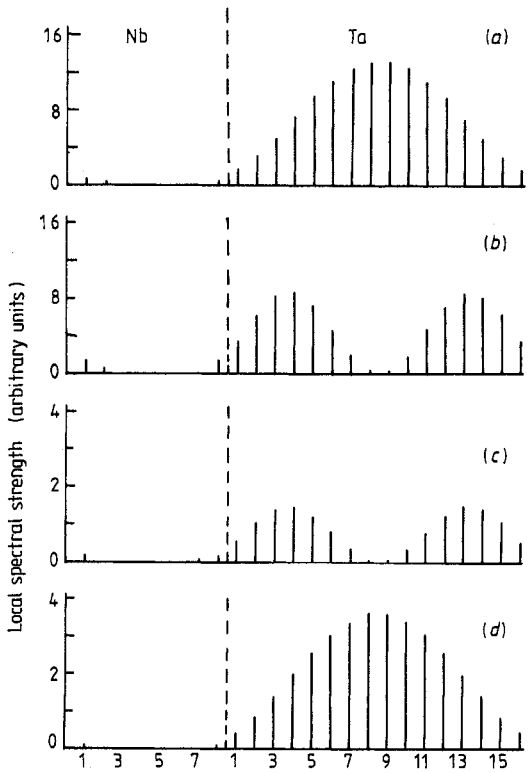

Figure 2. Spatial variation in the spectral strength (LDOS) for two high-energy states and two low-energy states at the Γ point of the Nb–Ta (001) (4, 8) superlattice for various energy eigenvalues: (*a*) 4.81 eV, (*b*) 4.68 eV, (*c*) −6.28 eV and (*d*) −6.44 eV.

Table 4. Energies of the highest and lowest electron states at Γ point in the Nb–Ta (001) $(N, 8)$ superlattices ($N = 2, 4, 8, 23$). Note that more states appear in the lower-energy range when N increases.

	E (eV)			
	$N = 2$	$N = 4$	$N = 8$	$N = 23$
Highest	4.81	4.81	4.81	4.81
Highest	4.79	4.78	4.78	4.78
Highest	4.68	4.68	4.68	4.68
Highest	4.51	4.55	4.56	4.56
Highest	4.32	4.49	4.49	4.49
Lowest	−5.71	−5.68	−5.69	−5.68
Lowest	−5.97	−5.70	−5.71	−5.72
Lowest	−6.05	−6.03	−6.02	−6.02
Lowest	−6.27	−6.28	−6.06	−6.06
Lowest	−6.41	−6.39	−6.28	−6.28
Lowest	−6.45	−6.44	−6.38	−6.38
Lowest	—	—	−6.44	−6.44

−1.32 eV and −1.16 eV) for the (4, 8) superlattice. In figure 3(*a*) the state is confined to Ta with a dip in the middle, as in figures 2(*b*) and 2(*c*). In figure 3(*b*) there is some leakage towards the Nb slab and more oscillations on the Ta side. In figure 3(*c*) there is a very strong accumulation towards the centre of the Nb slab and in figure 3(*d*) the spectral strength is evenly distributed between the two materials, with some oscillations across the entire period. Thus this marked variation in the spatial confinement of the different states appears in all energy ranges, near the Fermi level and far from it.

Exactly the same kind of behaviour has also been found for states near band edges for phonons in transition-metal superlattices [24] and electrons in semiconductor superlattices [8]. Thus this great diversity in spatial behaviour is independent of the specific type of state or elementary excitation. This is an inherently characteristic feature of the spectral phenomenology of superlattices which might significantly modulate some macroscopic properties of the composite superlattice system.

All the above results have been obtained by taking for the interaction parameters across the interface the mean of the two bulk values. We may expect these interactions to deviate somewhat from the arithmetic mean, although so far there is not yet any information available to throw light on this question for this kind of interface. We have studied the effect of changing these interactions to a weighted average, applying this to all ETB parameters involved and using weight factors 0.6–0.4. The results for the highest and lowest electron states at the Γ point of the (4, 4) superlattice are shown in tables 5 and 6. The number of confined bands remains unchanged and there are only very small shifts—upwards and downwards—of the eigenvalues, with no great changes otherwise, as was to be expected. In all these calculations, in order to obtain electron bands with sufficient accuracy, we added a small imaginary part to the energy ($E + i\eta$, where $\eta = 10^{-3}$ eV). This value of η was found convenient in practice.

4. Conclusions

We have obtained electron bands and the spatial variation in the spectral strength of different states for Nb–Ta (001) superlattices with different thicknesses of the constituent

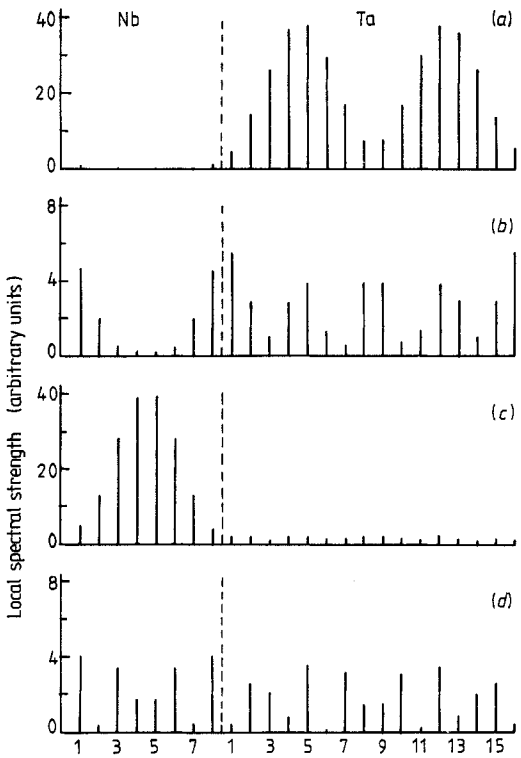

Figure 3. Same as figure 2 for four eigenstates of the same superlattice in the neighbourhood of the Fermi level for various energy eigenvalues: (*a*) −1.52 eV, (*b*) −1.38 eV, (*c*) −1.32 eV and (*d*) −1.16 eV.

Table 5. Energies of the highest and lowest electron states at the Γ point in the Nb–Ta (001) (4, 4) superlattice with weighting factors for the bulk interactions: 0.6 for Nb and 0.4 for Ta.

	E (eV)
Highest	4.73
Highest	4.66
Highest	4.39
Lowest	−5.88
Lowest	−6.22
Lowest	−6.34

slabs. The calculation is easily performed for ETB Hamiltonians using the SGFM method. A practical feature is that the increase in the number of layers of the constituents does not change the size of the matrices involved. For the ETB model used here, we have two atomic layers in a principal layer, five d orbitals in the basis (increasing the number of orbitals in the basis would not change the qualitative nature of the predictions obtained here, as was discussed before) and four principal layers involved between the two interfaces (l_B, l_A, r_A, r_B). This requires (40 × 40) matrices, irrespective of (N, N'). A direct diagonalisation of, for example, a (4, 8) superlattice would involve (120 × 120)

Table 6. Energies of the highest and lowest electron states at the Γ point in the Nb–Ta (001) (4, 4) superlattice with weighting factors for the bulk interactions: 0.4 for Nb and 0.6 for Ta.

	E (eV)
Highest	4.73
Highest	4.67
Highest	4.40
Lowest	−5.90
Lowest	−6.24
Lowest	−6.34

matrices. In this calculation, we have studied up to (23, 23) superlattices, with the same constant size, (40 × 40), of the secular matrix. Changes in the interactions between interface layers are also easily incorporated.

A significant feature of superlattices is the role of the thicknesses of the constituent materials. This can be followed by studying the evolution of the bands of confined states in different energy ranges. In this case the confined states are in the Ta slabs and they undergo considerable changes as N', the number of Ta principal layers, increases. Having a flexible method to repeat the calculation for different values of N', one can study the question of how much Ta is needed to form slabs of bulk Ta. This can be given a precise meaning in terms of the energies attained and the uniformity of the spatial distribution of all the confined states. It is seen that the macroscopic limit is attained very slowly. Even with $N' = 23$ (46 atomic layers) it is approximately, but not yet fully, reached.

The oscillatory behaviour found in figures 2 and 3 is analogous to that found for phonons in W–Mo superlattices [24] and electronic states in GaAs–AlAs superlattices [8]. This is seen to constitute a characteristic feature of superlattice states, irrespective of specific cases.

Acknowledgments

The authors would like to thank the International Center for Theoretical Physics (Trieste, Italy), for its hospitality, where part of this work was done. Two of the authors (RB and RAB-O) are indebted to the Dirección General de Investigación Cientifica y Técnica (Spanish Ministry of Education and Science) for a Sabbatical and Postdoctoral Research Fellowship, respectively, during which this work was carried out. This work was partly supported by the Comisión Interministerial de Ciencia y Tecnología (CICYT, Spain) under Grant MAT88-0547.

References

[1] Falco C M and Schuller I K 1982 *Superconductivity in d- and f-Band Metals* ed. W Buckel and W Weber (Karlsruhe: Kernsforschungsanslage) p 283

[2] Hertel G, McWhan D B and Rowell J M 1982 *Superconductivity in d- and f-Band Metals* ed. W Buckel and W Weber (Karlsruhe: Kernsforschungsanslage) p 299

[3] Freeman A J 1985 *Dynamical Phenomena at Surfaces, Interfaces and Superlattices* ed. F Nizzoli, K-H Rieder and R F Willis (Berlin: Springer) p 162
[4] Victora R H 1986 *Springer Proceedings in Physics* vol 14 ed. L M Falicov and J L Morán-López (Berlin: Springer) p 25
Victora R H and Falicov L M 1985 *Phys. Rev.* B **31** 7335
[5] García-Moliner F and Velasco V R 1986 *Phys. Scr.* **34** 252
[6] García-Moliner F and Velasco V R 1986 *Prog. Surf. Sci.* **21** 93
[7] López-Sancho M P, López-Sancho J M and Rubio J 1984 *J. Phys. F: Met. Phys.* **14** 1205; 1985 *J. Phys. F: Met. Phys.* **15** 851
Baquero R *ICTP preprint* ICTP/88/185
[8] Muñoz M C, Velasco V R and García-Moliner F 1989 *Phys. Rev.* B **39** 1786
[9] Velasco V R, García-Moliner F, Miglio L and Colombo L 1988 *Phys. Rev.* B **38** 3172
[10] Baquero R, Velasco V R and García-Moliner F 1988 *Phys. Scr.* **38** 742
[11] Harrison W A 1980 *Electronic Structure and the Properties of Solids* (San Francisco, CA: Freeman)
[12] Papaconstantopoulos D A 1986 *Handbook of the Band Structure of Elemental Solids* (New York: Plenum)
[13] Djafari-Rouhani B, Dobrzynski L and Masri P 1985 *Phys. Rev.* B **31** 7379
[14] Priester C, Allan G and Lannoo M 1986 *Phys. Rev.* B **33** 7386
[15] Haussy B, Priester C, Allan G and Lannoo M 1987 *Phys. Rev.* B **36** 1105
[16] Platero G, Sánchez-Dehesa J, Tejedor C and Flores F 1986 *Surf. Sci.* **168** 553
[17] Muñoz A, Durán J C and Flores F 1987 *Surf. Sci.* **181** L200
[18] Ren S Y and Dow J D 1988 *Phys. Rev.* B **38** 1999
[19] Froyen S 1989 *Phys. Rev.* B **39** 3168
[20] Quiroga L, Camacho A and Baquero R to be published
[21] Falco C M, Bennett W R and Boufelfel A 1985 *Dynamical Phenomena at Surfaces, Interfaces and Superlattices* ed. F Nizzoli, K H Rieder and R F Willis (Berlin: Springer) p 35
[22] Brito-Orta R A, Velasco V R and García-Moliner F 1987 *Surf. Sci.* **187** 223
[23] Fernandez L, Velasco V R and García-Moliner F 1987 *Surf. Sci.* **188** 140
[24] Brito-Orta R A, Velasco V R and García-Moliner F 1988 *Phys. Rev.* B **38** 9631